Caliphate Journal of Science & Technology (CaJoST)

[1]Department of Chemistry, Sokoto State University, Sokoto, Nigeria.
[2]Department of Pure and Environmental Chemistry, Usmanu Danfodiyo University, Sokoto, Nigeria.
[3]Department of Energy and Applied Chemistry, Usmanu Danfodiyo University, Sokoto, Nigeria.
[4]School of Chemical Engineering, Universiti Sains Malaysia, Penang, Malaysia.

*Corresponding author's email:

yakubu.muhammadsahabi@ssu.edu.ng

Molecular Profile, Fuel Properties, Engine Performance and Emission Characteristics of Gasoline-Like Fuel Produced Via Cracking of Used Engine Oil Using Na-Fe$_3$O$_4$/HZSM-5 Catalyst

Yaquba M. Sahabi[*1,3], Abdullahi M. Sokoto[2], Misbahu L. Mohammed[3], Abdul Rahman Mohamed[4]

A vast quantity of used engine oil (UEO) is generated every day and poses a major disposal issue in modern society due to the heavy metals and other hazardous contaminants present in it. Due to its high carbon content, UEO has great potential to be utilized as a feedstock for fuel production. The studies on the molecular profile, fuel properties, engine characteristics of gasoline-like fuel produced via cracking of UEO were conducted. The Fe$_3$O$_4$ nanoparticles was synthesized via the one-spot method using iron (III) chloride hexahydrate (FeCl$_3$.6H$_2$O) and iron (II) chloride tetrahydrate (FeCl$_2$.4H$_2$O) as precursors, while the HZSM-5 was synthesized using Al$_2$(SO$_4$)$_3$.18H$_2$O and Na$_2$SiO$_3$ as sources of alumina and silica, respectively. The UEO was cracked in a fixed stainless-steel batch reactor for 1h at varying temperature (350 – 450 ºC). The liquid fuel product obtained was analysed for its molecular composition using GC-MS and FTIR, while ASTM standard procedure was used to determine the fuel properties. The results showed that the catalyst is 97.60% selective for gasoline range hydrocarbons, which could be attributed to the high surface area of HZSM-5, which offers more active sites for catalytic cracking. The fuel properties of the produced liquid fuel determined include specific gravity (0.76), kinematic viscosity (1.69 mm^2/Sec), flash point (-42 °C), auto ignition temperature (225 °C), carbon residue (0.12%), lower heating value (40,443 KJ/kg), and octane number (94). The engine characteristics results of the liquid fuel were comparable to those of commercially available gasoline. Based on the results obtained, it was concluded that the fuel obtained could be used directly in spark-ignition engines without any negative impact on engine performance.

Keywords: Engine oil, Gasoline, Cracking, Catalyst.

1. Introduction

With the rapid development of the automotive industry and the improvement in living standards, the number of vehicles and electrical energy-generating sets owned by individuals and industries has increased dramatically throughout the world (Zhang *et al.,* 2017). Consequently, used engine oil (UEO) has become one of the most abundant waste materials. It has been estimated that throughout the world, an average of 24 million metric tonnes of UEO are generated every year, which poses a significant disposal issue for modern society (Zandi-Atashbar *et al.,* 2017). UEO also poses an environmental hazard due to the harmful contaminants present in it, such as heavy metals, polychlorinated biphenyls, and polycyclic aromatic hydrocarbons. In recent years, the conversion of UEO to fuels and other valuable chemicals has become an important topic for researchers. Consequently, various conversion methods have been employed to convert UEO into useful products, including solvent extraction, gasification, hydrogenation, hydrothermal processing, pyrolysis, etc. (El-Mekkawi *et al.*, 2020; Moses *et al.,* 2023). However, there are limitations to these methods, such as high reagent demand, high energy demand, high operational cost, time consumption, and the formation of undesired products (Pinheiro *et al.*, 2017; El-Mekkawi *et al.*, 2020).

Nowadays, thermo-catalytic cracking is considered the simplest and most effective

technique for producing liquid fuel under the combined action of suitable catalysts and thermal energy (Alavi *et al.*, 2019; Mishra *et al.*, 2021; Balboul *et al.,* 2022; Moses *et al.,* 2023). Compared with other energy recovery methods, catalytic cracking works by using uniform volume heating from the inside out. It has advantages such as low operational cost, isomerization of smaller gaseous fragments into gasoline-range hydrocarbons, a lower catalyst-to-oil ratio, producing gasoline with a high octane rating that burns cleanly, lowering the proportion of higher hydrocarbon fuel oils, fuel that can be used without any additives as it is a pure hydrocarbon, can be applied on industrial scales, and relatively environmentally friendly (Santhoskumar and Ramanathan, 2020; Mishra *et al.*, 2021; Balboul *et al.,* 2022). Therefore, kinetic optimization of this method to recover high-quality fuel from UEO and reduce its harm to the environment has become a research hotspot for many researchers (Ramanathan and Santhoskumar, 2020). Finding an appropriate catalyst that can modify the reaction parameters of the process to lower the temperature and time of the reaction has been the focus of recent studies (Alavi *et al.*, 2019). The thrust of the present study is to investigate the molecular profile, fuel properties, engine performance, and emission characteristics of gasoline-like fuel produced via cracking of used engine oil using Na-Fe$_3$O$_4$/HZSM-5 catalyst.

2. Materials and Methods

2.1 Materials

UEO was collected at Total Automobile Lube Workshop, Western Bypass, Sokoto, Nigeria. The UEO was collected in a cleaned gallon directly from the car engine after the vehicle has been driven for an approximate range of 2000 km. Prior to the cracking, the UEO sample was filtered to remove carbon soot and other solid impurities such that the size of any remaining particulates was less than 50 μm. Aluminium sulphate octadecahydrate [Al$_2$(SO$_4$)$_3$.18H$_2$O], sodium silicate (Na$_2$SiO$_3$), Iron (III) chloride hexahydrate (FeCl$_3$.6H$_2$O, 31.62 g) and iron (II) chloride tetrahydrate (FeCl$_2$.4H$_2$O, 12.54 g), sulphuric acid (H$_2$SO$_4$), hydrochloric acid (HCl), and sodium hydroxide (NaOH) were purchased from Sigma-Aldrich.

2.2 Methods

2.2.1 Synthesis of Iron Fe$_3$O$_4$ Nanoparticles

The Fe$_3$O$_4$ nanoparticles was prepared by a one-pot synthesis method. A mixture of iron (III) chloride hexahydrate (FeCl$_3$.6H$_2$O, 31.62 g) and iron (II) chloride tetrahydrate (FeCl$_2$.4H$_2$O, 12.54 g) was added to a solution of hydrochloric acid (0.41 mol/dm^3, 150 cm^3) with continuous stirring until a clear solution is formed. In the solution, sodium hydroxide (1.5 mol/dm^3) was added in dropwise with constant stirring at 60 °C until an instant black precipitate is generated. The pH value of final suspension was maintained at 10. The resulting suspension was stirred for about 1h using hot plate magnetic stirrer. The product formed was separated by a magnet and then washed once distilled with 800 cm^3 deionized water to obtain Fe$_3$O$_4$ nanoparticles modified with certain content of residual sodium. The freshly made nanoparticles was dried overnight at 60 °C (Wei *et al.,* 2017; Aragaw *et al.*, 2021).

$$FeCl_2.4H_2O + 2FeCl_3.6H_2O + 8NaOH \longrightarrow Fe_3O_4 + 8NaCl + 20H_2O$$
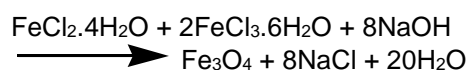
2.2.2 Synthesis of HZSM-5

First, solution A as the source of alumina was prepared. The solution contained 26.7 g of aluminium sulphate (Al$_2$(SO$_4$)$_3$.18H$_2$O), 56 g of 98% sulphuric acid (H$_2$SO$_4$), and 15 cm^3 of deionized water. After that, solution B as the source of silica was prepared. The solution contained 56 g of sodium silicate (Na$_2$SiO$_3$) and 56 g of 40% (w/v) sodium hydroxide (NaOH). Solution A and Solution B were slowly mixed together. The mixture was then homogenized using a magnetic stirrer at a speed of 1200 rpm for 5 minutes. The crystallization was performed in static conditions at 180 °C for 48 hours using a stainless steel teflon-lined autoclave in an air oven. The solid product was recovered by filtration, washed several times with deionized water until the pH of the decanted water was 7, and then dried overnight at 105 °C. Finally, the catalyst sample was calcined to remove the organic template in a muffle furnace under an air flow at 530 °C for 12 hours at a heating rate of 3 °C/minute. The ZSM-5 zeolite in hydrogen form (H-ZSM-5) was obtained through ion exchange with an aqueous NH$_4$NO$_3$ solution. (Veses *et al.,* 2016; Widayat and Anissa, 2016; Niu *et al.,* 2017).

2.2.3 Catalyst Doping

The doping of 5 wt.% Na-Fe$_3$O$_4$ on HZSM-5 was performed by mixing a solution containing 10 g of the Fe$_3$O$_4$ nanoparticles with 95g HZSM-5 catalyst support on a magnetic stirrer at 1000 rpm for 15 min. After doping, the catalyst sample was dried at 105 °C for 4 h and calcined at 700 °C for 4 h (Wei *et al.,* 2017).

2.2.4 Cracking of the Used Engine Oil

The cracking of the UEO was carried out in a fixed bed stainless steel reactor equipped with a

pressure gauge. The composite catalyst (1g) was placed on the catalyst bed and the UEO (100 cm³) was poured into the reactor. The reactor was closed tightly and then mounted on a tubular-electric furnace equipped with thermo couples. The condenser inlet was then connected to the reactor outlet, and all the reaction conditions were set. The cracking was carried out at varying temperature (350 – 450 ºC) for 1h. After the completion of the reaction, the outlet valve was gradually opened to vent out the vapour products. The product was condensed using the water condenser and was collected at the bottom of the condenser for analysis.

2.2.5 Analysis of UEO and Produced Liquid Fuel

ASTM standard methods were followed to determine the fuel properties of the liquid product, while GC-MS and FTIR were used to examine the molecular profile and functional groups respectively, of the UEO and liquid products.

2.2.6 Catalyst Reusability Test

After the cracking of the UEO, the solid catalyst was separated from the liquid using filter paper and washed with methanol and n-hexane to remove polar and non-polar compounds, respectively. The solid catalyst recovered was further washed with distilled deionized water and then dried at 105 °C for 1 hour to remove water content. It was then finally calcined at 700 °C for 3 hours in an electrically heated furnace (Istadi *et al.,* 2016; Madhu and Sharma, 2017). The regenerated catalyst was then used for the cracking of UEO for 5 consecutive cycles to determine its reusability with regeneration by washing and thermal treatment to determine its reusability.

2.2.7 Engine Performance and Exhaust Emission Analysis

The engine performance and emission characteristics of the produced liquid fuel and commercially available gasoline were carried out on a four stroke, single cylinder, carbureted, spark ignition (SI) engine. The engine was modified from an original spark ignition motorcycle engine that was used in real vehicles and is equipped with a dynamometer, a fuel measurement system, and an exhaust gas analyzer.

3. Results and Discussion

3.1 Molecular Composition of the Produced Fuel

Gasoline fuel is a complex mixture of varieties of classes of hydrocarbons, mainly paraffins, olefins, naphthenes, and aromatics, ranging between C_4 - C_{12} carbon atoms with a boiling range of 30 – 225°C. (Gong, 2022; Suiuay *et al.,* 2023). The fuel properties of gasoline affect the combustion process because fuel/air mixture oxidation is controlled by the fuel molecular composition (Sarathy *et al.,* 2017). The molecular compositions of the produced liquid fuel are shown in Table 1, While carbon number and PONA distributions (percentage) are shown in Figure 1 and Figure 2, respectively.
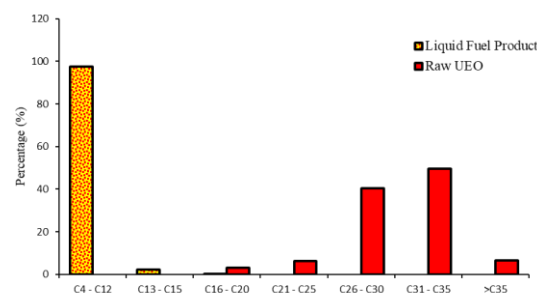
Figure 1: Carbon Range Distribution in Produced Liquid Fuel.
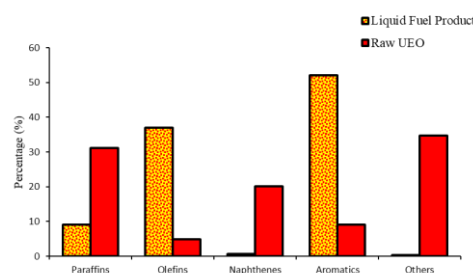
Figure 2: PONA Distribution in Produced Liquid Fuel.

Table 1: Molecular Composition of the Liquid Product

S/N	Retention Time	Area Percentage	Compounds	Carbon Number	Quality (%)
1.	10.6755	0.4408	(1-Methylbuta-1,3-dienyl)-benzene	C_{11}	55
2.	7.8626	0.4362	(3-Methylphenyl) methanol, neopentyl ether	C_{13}	72
3.	6.328	0.3322	1,2-Bis(3-cyclohexenyl)-ethylene	C_{14}	78
4.	5.5346	7.8532	1,3,8-p-Menthatriene	C_{10}	51
5.	13.9059	0.616	1,4,4a,5,8,8a-Hexahydro-naphthalene	C_{10}	72

6.	7.6503	4.9923	1-methyl-1H-Indene	C_{10}	81
7.	8.3453	1.4171	1-methylene-1H-Indene	C_{10}	60
8.	8.6419	0.5493	2,3-dihydro-1,6-dimethyl-1H-Indene	C_{11}	94
9.	10.2442	0.6577	2,3-dihydro-4,7-dimethyl-1H-Indene	C_{11}	95
10.	9.7793	0.2369	2-Ethyl-2,3-dihydro-1H-indene	C_{11}	74
11.	5.6436	25.9573	3a,4,5,6,7,7a-Hexahydro-4,7-methanoindene	C_{10}	93
12.	7.309	0.8332	3-Phenylbut-1-ene	C_{10}	93
13.	6.2275	8.4953	Octahydro-4,7-Methano-1H-indene	C_{10}	90
14.	13.7191	0.9946	4-Pentyn-1-ol	C_5	46
15.	8.4063	2.1308	(1,1-dimethylpropyl)- Benzene	C_{11}	87
16.	19.8708	4.4652	(2-methyl-1-butenyl)- Benzene	C_{11}	94
17.	7.5638	3.9691	(2-methyl-1-propenyl)- Benzene	C_{10}	90
18.	6.8639	0.4792	1,2,3,4-tetramethyl- Benzene	C_{10}	95
19.	6.9691	1.4605	1,2,4,5-tetramethyl- Benzene	C_{10}	96
20.	7.6856	3.3351	1-ethyl-2,3-dimethyl- Benzene	C_{10}	94
21.	5.979	1.9883	1-methyl-3-(1-methylethyl)- Benzene	C_{10}	64
22.	5.3294	1.6153	1-methyl-3-propyl- Benzene	C_{10}	94
23.	10.5629	1.2342	2-ethenyl-1,3,5-trimethyl- Benzene	C_{11}	83
24.	6.144	3.078	4-ethyl-1,2-dimethyl- Benzene	C_{10}	93
25.	10.7268	1.0033	Hexyl- Benzene	C_{12}	43
26.	6.4862	0.1935	2-methyl- Bicyclo[2.2.1]hept-2-ene	C_8	78
27.	9.6528	0.2694	Dodecane	C_{12}	89
28.	8.2651	6.1781	Naphthalene	C_{10}	95
29.	10.8982	1.4037	1,2,3,4-tetrahydro-5,7-dimethyl- Naphthalene	C_{12}	80
30.	22.7479	8.5662	1-methyl- Naphthalene	C_{11}	97
31.	13.7653	1.5517	2-ethyl-Naphthalene	C_{12}	95
32.	5.4385	2.5952	p-Mentha-1,5,8-triene	C_{10}	74
33.	29.7399	0.313	Trans-13-Octadecenoic acid	C_{18}	99
34.	12.3492	0.3582	Tridecane	C_{13}	94

As shown in Figure 1 the carbon number distribution was relatively wide in the raw UEO, and it was distributed in C_{16} – C_{35}, and primarily concentrated in C_{26} – C_{35} by 90.12%. After thermal cracking with Na-Fe$_3$O$_4$/HZSM-5, the distribution of carbon number became narrower, and its peak tended to shift to lower carbon number (C_5 - C_{12}) by 97.60%. This showed that the catalyst helped to convert the heavy hydrocarbon components in the UEO into lighter components with lower carbon number similar to conventional gasoline. The selectivity of hydrocarbons was related to the satisfactory pores and active acid sites of the HZSM-5, where larger molecules in the UEO can enter and interact with the Lewis and Bronsted acid sites in the pores, thus leading to C – C bond breakage and light components with lower carbon numbers being generated. Paraffins, naphthenes and non-hydrocarbons (including oxygenates and organic halides) are dominant in the UEO with a respective composition of 31.09%, 20.02% and 34.74%. However, upon thermal cracking with Na-Fe$_3$O$_4$/HZSM-5, the PONA distribution was significantly altered with selectivity towards olefins (37.03%) and aromatics (52.09%). This indicates that catalyst incorporation controls the PONA distribution in UEO cracking which is in support to the previous reports (Dwivedi *et al.*, 2021).
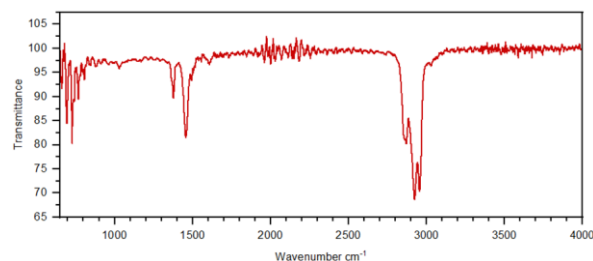
Figure 3: FTIR Spectrum of the Produced Liquid Fuel

The FT-IR spectrum of the liquid product was recorded in the frequency range of 4000 – 650 cm^{-1}. The C – H stretching vibrations of paraffins were detected in the frequency range of 2990 – 2850 cm^{-1}. The presence of strong intensity

peaks indicates that the paraffin content is high across all the samples. The strong peaks displayed at 1440 cm^{-1} represent the C=C stretching vibration in aromatics. The aromatics and olefins as constituents of the gasoline-like fuels under study were ensured by the appearance of some medium intensity peaks within the frequency range of 840 – 650 cm^{-1} due to =C-H bending (out plane) vibration.

3.2   Effect of Temperature on Product Selectivity

Figure 4 shows the effects temperature on gasoline range hydrocarbons and PONA selectivity.

P = Paraffins, O = Olefins, N = Naphthenes, A = Aromatics
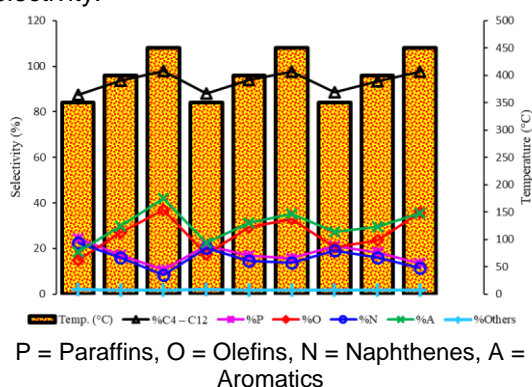
Figure 4: Effect of Temperature on Product Selectivity

The cracking experiments were conducted at a temperature range of 350 – 450ºC. It could be noted from Figure 4 that, in the cracking process, temperature is an effective parameter on the product's carbon range and PONA selectivity. The three highest conversions of UEO to gasoline range hydrocarbons were achieved at 450 °C and different catalyst loading and time combinations. It can also be seen from the results that the selectivity of gasoline range hydrocarbons, olefins and aromatics increased as the temperature increased. From the results, it can be said that cracking, olefination, and aromatization reactions are more effective as the temperature increases. The increase in selectivity of the catalyst with temperature could be attributed to the opening of the catalyst's sites at high temperature, resulting in the availability of more catalyst's active sites, which promote conversion (Balboul *et al.,* 2022). Also, it could be due to the increase in the number of higher energy free radicals at high temperatures (Mousavi *et al.,* 2022). Lower temperatures may lead to a significant amount of residual coke being accumulated on the catalyst's active sites and surface area, which could result in catalyst deactivation. A similar trend of increased conversion at higher temperatures was reported by Balboul *et al.* (2022) for liquid fuel obtained via catalytic cracking of used sunflower oil catalysed by Praseodymium-supported alumina.

In a similar scenario, El-Deeb *et al.* (2022) reported that light hydrocarbons exhibited a linear increase with elevating the temperature, which indicated the higher cracking activity for gasoline and diesel-like fuel obtained via hydrocracking of hydrotreated tyre pyrolytic oil over Ni-W/MCM-41 derived from blast furnace slag.

3.3   Fuel Properties of the Produced Fuel

Understanding the properties of fuels like gasoline is very critical to ensure the normal operation of internal combustion engines with regards to processes like spray atomization, heating, evaporation etc (AlNazar *et al.,* 2023). The measured properties of the produced liquid fuel are shown in Table 2. The results obtained reveal that most of the fuel properties of the produced liquid fuel are very similar to those of commercially available gasoline.

Table 2: Fuel Properties of Produced Liquid Fuel Vs. Commercially Available Gasoline

Parameter	Produced Liquid Fuel	Commercially Available Gasoline
Specific Gravity	0.76	0.72
Kinematic Viscosity (mm^2/Sec)	1.69	0.164
Lower Heating Value (KJ/kg)	40,433	44,340
Carbon Residue (wt.%)	0.12	0.08
Cloud Point (ºC)	-55	-64
Flash Point (ºC)	-42	-53
Auto ignition Temperature (ºC)	225	204
Octane Number	94	93
Sulphur Content (wt.%)	ND	ND
Water Content (wt.%)	ND	ND

ND = Not detected

3.4   Catalyst Reusability

Regeneration is one of the important property indicators of a good catalyst. The Na-Fe$_3$O$_4$/HZSM-5 catalyst was tested for its reusability over five consecutive cycles of usage after the regeneration process (washing and thermal treatment). The result of catalyst reusability for the cracking reactions is shown in Figure 5.
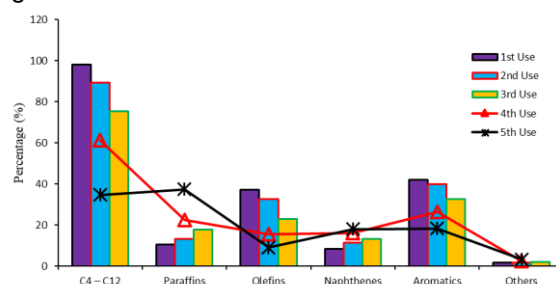
Figure 5: Catalyst Reusability Test

The results in Figure 5 indicated that the catalyst has almost consistent activity up to four cycles of usage after simple regeneration. The decreasing catalytic activity during the fifth repeating usages may be probably due to; poisoning of the catalyst active sites, collapsing of the catalyst's structure and coke deposition on the HZSM-5 pore (which reduced the frequency of interaction between the active sites and reactants). The first run gave the highest yield of 97.9% gasoline range hydrocarbon, but in the case of the second run, the reused catalyst gave 89.4% gasoline range hydrocarbon. After subsequent regeneration and reuse, the catalyst yields 75.4%, 61.1%, and 34.7% gasoline range hydrocarbons for the third, fourth, and fifth runs, respectively. In the reusebility test, no loss in catalyst weight was observed after the completion of the reactions.

3.5 Engine Performance and Exhaust Emission Analysis

The performance and emissions of the engine running on the produced liquid fuel was evaluated and compared with commercially available gasoline fuel. Altogether, there is a considerable similarity in engine performance and emissions characteristics between the synthesised fuel product and commercially available gasoline fuel. The fuels were tested under varying engine speed (rpm) conditions. The brake power, basic specific fuel consumption (BSFC), exhaust temperature, and exhaust gas emissions (CO, CO_2, and HC) of the engine were recorded against the engine speed (rpm).

3.5.1 Brake Power

The *brake power (*is sometimes referred to as engine output power*)* of an internal combustion engine is the power available at the crankshaft for doing useful work and is measured with the help of a dynamometer. Figure 6 presents the effects of engine speed on brake power using the produced liquid fuel and commercially available gasoline fuels. It can be observed from the figure that the tendency of power for the two fuels is similar.
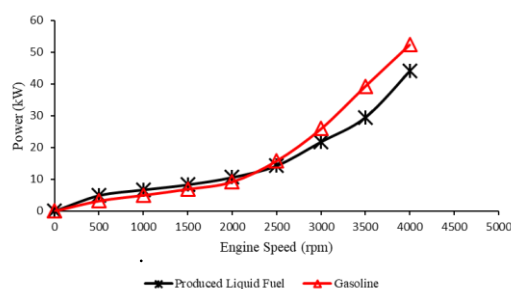
Figure 6: Brake Power of Synthesised Fuel vs. Commercially Available Gasoline.

The results from Figure 6 showed that the engine brake power increases steadily up to 4000 rpm for the two fuels. The maximum engine brake power recorded at 4000 rpm is 44.1 kW and 52.4 kW for the produced liquid fuel and commercially available gasoline fuel, respectively. The low brake power of the produced liquid fuel may be associated to the lower calorific value, poor volatility, and poor combustion characteristics of biodiesel compared to commercially available gasoline (Gad and Ismail, 2021).The steady increase in power with engine rpm is consistent with that reported by Elfasakhany (2016) and Najafi *et al.* (2015) for acetone-gasoline fuel blends and gasoline-ethanol blends in spark ignition engines, respectively.

3.5.2 Exhaust Gas Temperature (EGT)

Figure 7 shows exhaust gas temperature trends for the synthesised fuel and commercially available gasoline fuel.
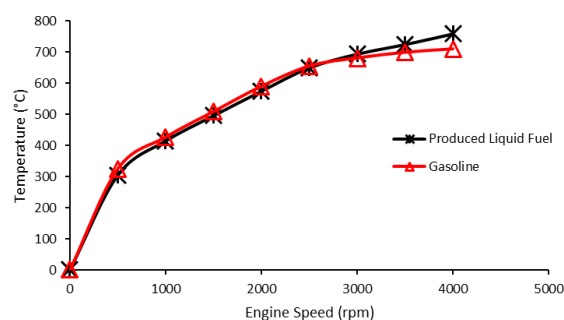
Figure 7: EGT of Synthesised fuel vs. Commercially Available Gasoline.

As depicted, the exhaust gas temperature increases with an increase in the engine speed for the two test fuels. At higher engine speeds (between 3000 – 4000 rpm), the engine fueled with commercially available gasoline shows the highest exhaust gas temperature, compared to produced liquid fuel. The reason for the difference in exhaust temperature could be due to the difference in lower heating value of the of fuels under test (Cesur, 2022). This trend of increasing temperature with engine speed is similar to those reported by Prayogi *et al.* (2019) and Cesur (2022) for gasoline engine fueled by gasoline-acetone-wet methanol blends and ethanol fueled gasoline engine, respectively.

3.5.3 Brake Specific Fuel Consumption (BSFC)

Brake specific fuel consumption (BSFC) is an important parameter to compare the performance of synthesized fuel and gasoline fuel on an

engine. Figure 8 shows the BSFC (kg/kWh) results of the test fuels.
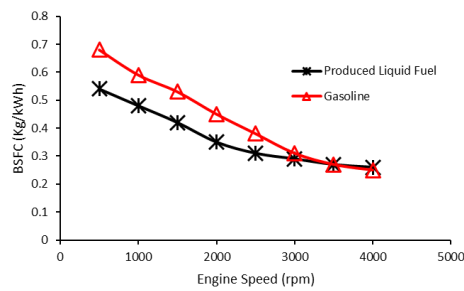
Figure 8: BSFC of Synthesised fuel vs. Commercially Available Gasoline.

As seen in Figure 8, the BSFC values decreased with increasing engine speed (rpm). At the onset of the experiment, the produced liquid fuel had a higher BSFC than that of the commercially available gasoline fuel. This could be due to the lower heating value of the produced liquid fuel, so the engine consumes extra fuel when operated with synthesised fuel to develop the same power (Gad and Ismail, 2021). The measured heating value of produced liquid fuel is 40,433 KJ/kg, while that of commercially available gasoline fuel is about 44,340 KJ/kg. A similar trend of high BSFC associated with low LHV was reported by Gad and Ismail, (2021) for waste cooking oil biodiesel.

3.5.4   Carbon Monoxide (CO) Emission

CO is a colourless, odorless, and toxic exhaust gas, and it is one of the indicators of incomplete combustion of fuels. The CO gas emission results obtained from the test fuels are shown in Figure.9.
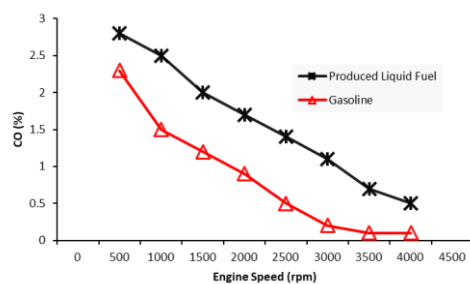
Figure 9: CO Emissions of Synthesised Fuel vs. Commercially Available Gasoline

It can be seen from Figure 9 that throughout the experiment, the CO gas emission of the produced liquid fuel was a bit higher than that of commercially available gasoline. When the engine speed was increased to higher rpm, CO emissions decreased. The decrease in CO gas emission at higher engine power could be attributed to the increase in engine temperature,

which promotes the complete combustion of fuels (Hosseini et al., 2023). Moreover, compared to pure gasoline, the produced liquid fuel contains oxygenates, which may contribute to a complete combustion and thus better conversion of CO to CO_2. Simsek et al. (2020) observed similar decreases in CO emissions at higher engine power for gasoline-LPG-biodiesel blends in different volumetric percentages in a single cylinder, four-stroke, spark ignition (SI) engine with different throttle positions. Similarly, Hosseini et al. (2023) reported a 23.46% decrease in CO gas emission at full engine load for an ethanol-gasoline fuel blend.

3.5.5   Carbon dioxide (CO_2) Emission

The main component of exhaust emissions built up by burning hydrocarbon-based fuels is CO_2 emissions. The CO_2 emissions of most fuels depend on the carbon content as well as the H/C ratio. A higher H/C ratio results in lower CO_2 emissions with increased fuel power, and vice versa (Suiuay et al., 2020). CO_2 gas is one of the greenhouse gases. Figure 10 shows the variation in CO_2 emissions of the produced liquid fuel and commercially available gasoline fuel at different engine speeds (rpm).
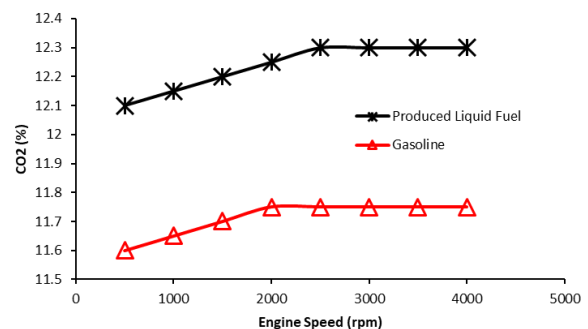
Figure 10: CO_2 Emission of Synthesised Fuel vs. Commercially Available Gasoline

From Figure 10, it is apparent that the amount of CO_2 concentration is higher for produced liquid fuel compared to that for commercially available gasoline. CO_2 gas emissions were observed to increase with increasing engine speed from 500 to 2500 rpm. While at higher rpm, the CO_2 gas emission remains steady for all the test fuels. A similar trend was reported by Prayogi et al. (2019) for gasoline engine fueled by gasoline, acetone, and wet methanol blends.

3.5.6   Unburnt Hydrocarbon (UHC) Emission

The emitted UHC mainly consists of unburned fuel and is resulted from quenching flames, deposits, and the desorption of fuel out of the engine oil (Alptekin et al., 2017). UHC emissions

depend on fuel type, the geometry of the combustion chamber, and engine operating conditions (Alptekin *et al.,* 2017). Figure 11 shows the variation in concentration of UHC emissions for the synthesised fuel and commercially available gasoline at different engine speeds.
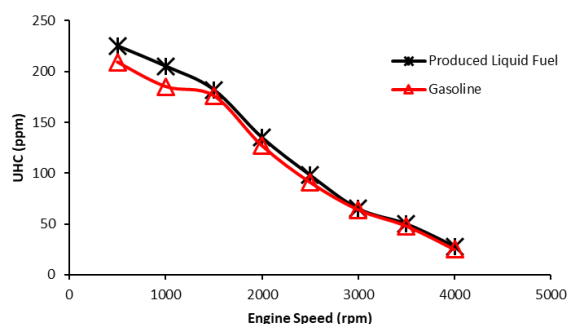
Figure 11: UHC Emission of Synthesised Fuel vs. Commercially Available Gasoline

It can be observed from Figure 11 that UHC emissions for the two fuels have similar trends, which increase at lower rpm and then decrease significantly at engines at higher rpm. A similar trend was reported by Deng *et al.* (2018) for a spark ignition engine fueled with pure gasoline and hydrous ethanol-gasoline blends.

4. Conclusion

In the present study, molecular profile, fuel properties, engine performance and emission characteristics of gasoline-like fuel produced via cracking of UEO was studied. The results of molecular profile and fuel properties confirmed the production of high-quality fuels with properties similar to conventional gasoline fuel, which can be used as an alternative in gasoline engines. The Na-Fe$_3$O$_4$/HZSM-5 catalysts exhibited a higher catalytic performance due to their higher surface area, pore size and volume, strong acidity, good dispersion in the reaction medium, and good metal-support interaction. The overall study suggests that iron oxide nanoparticles promoted with over HZSM-5 support could be a suitable catalyst for the enhanced and cost effective production of highly sustainable gasoline fuel from UEO.

Conflict of interest
The authors declare no conflict of interest.

Acknowledgements

References

Alavi, S. E., Abdoli, M. A., Khorasheh, F. and Bayandori Moghaddam, A. (2019). Evaluation of Catalytic Effects of Metal Oxide Nanoparticles on Pyrolysis of Used Lubricating Oil. *Pollution*, *5*(4), 879–893. https://doi.org/10.22059/poll.2019.272588.5 60

Alptekin, E. and Canakci, M. (2017). Performance and emission characteristics of solketal-gasoline fuel blend in a vehicle with spark ignition engine. *Applied Thermal Engineering*, *124*, 504–509. https://doi.org/10.1016/j.applthermaleng.201 7.06.064

Aragaw, T. A., Bogale, F. M. and Aragaw, B. A. (2021). Iron-based nanoparticles in wastewater treatment: A review on synthesis methods, applications, and removal mechanisms. *Journal of Saudi Chemical Society*. (2021) 25. 101280. https://doi.org/10.1016/j.jscs.2021.101280

Balboul, B. A. A., Abdelrahman, A. A., Salem, H. M., Mohamed, E. A., Osman, D. I. and Rabie, A. M. (2022). Enhanced production of liquid fuel via catalytic cracking of used sunflower oil catalyzed by Praseodymium supported alumina. *Journal of Molecular Liquids*, 367 367 (2022) 120562. https://doi.org/10.1016/j.molliq.2022.120562

AlNazr, H. A., Ahmad, N., Ahmed, U., Mohan, B. and Jameel, A. G. A. (2023). Predicting physical properties of oxygenated gasoline and diesel range fuels using machine learning. *Alexandria Engineering Journal*. 76 (2023). 193 – 219. https://doi.org/10.1016/j.aej.2023.06.037

Cesur, I. (2022). Effects of water injection strategies on performance and exhaust emissions in an ethanol fueled gasoline engine. *Thermal Science and Engineering Progress*, *34* (March), 101397. https://doi.org/10.1016/j.tsep.2022.101397

Deng, X., Chen, Z., Wang, X., Zhen, H. and Xie, R. (2018). Case Studies in Thermal Engineering Exhaust noise, performance and emission characteristics of spark ignition engine fuelled with pure gasoline and hydrous ethanol gasoline blends. *Case Studies in Thermal Engineering*, *12*(February). 55–63. https://doi.org/10.1016/j.csite.2018.02.004

Dwivedi, U., Naik, S. N. and Pant, K. K. (2021). High quality liquid fuel production from waste plastics via two-step cracking route in a bottom-up approach using bi-functional Fe/HZSM-5 catalyst. *Waste Management*. 132(2021). 151 – 161.

https://doi.org/10.1016/j.wasman.2021.07.024

El-Deeb, Z. M., Aboutaleb, W. A., Mohamed, R. S., Dhmees, A. S., and Ahmed, A. I. (2022). Gasoline and diesel-like fuel production via hydrocracking of hydrotreated tire pyrolytic oil over Ni-W/MCM-41 derived from blast furnace slag. *Journal of the Energy Institute*, *103*, 84–93. https://doi.org/10.1016/j.joei.2022.05.013

Elfasakhany, A. (2016). Engineering Science and Technology, an International Journal Performance and emissions analysis on using acetone – gasoline fuel blends in spark-ignition engine. *Engineering Science and Technology, an International Journal*, *19*(3), 1224–1232. https://doi.org/10.1016/j.jestch.2016.02.002

El-Mekkawi, S. A., El-Ibiari, N. N., Attia, N. K., El-Diwani, G. I., El-Ardy, O. A. and Morsi, A. K. E. (2020). Reducing the Environmental Impact of Used Lubricating Oil Through the Production of Fuels by Pyrolysis. *Environmental Nanotechnology, Monitoring and Management*, *14*, 100308. https://doi.org/10.1016/j.enmm.2020.100308

Gad, M. S. and Ismail, M. A. (2021)., Effect of Waste Cooking Oil Biodiesel Blending with Gasoline and Kerosene on Diesel Engine Performance, Emissions and Combustion Characteristics. *Process Safety and Environmental Protection*. 149 (2021) 1–10. https://doi.org/10.1016/j.psep.2020.10.040

Gong, J. (2022). Study on Preparation of Fuel Oil from Three Kinds of Molecular Sieve Catalytic Cracking Waste Lubricating Oil. *Journal of Physics: Conference Series*, *2168*(1). https://doi.org/10.1088/1742-6596/2168/1/012010

Hosseini, H., Hajialimohammadi, A., Gavzan, I. J. and Hajimousa, M. A. (2023). Numerical and experimental investigation on the effect of using blended gasoline-ethanol fuel on the performance and the emissions of the bi-fuel Iranian national engine. *Fuel*, *337*(August 2022), 127252. https://doi.org/10.1016/j.fuel.2022.127252

Istadi, I., Mabruro, U., Kalimantini, B. A. and Buchori, L. (2016). Reusability and Stability Tests of Calcium Oxide Based Catalyst (K_2O/CaO-ZnO) for Transesterification of Soybean Oil to Biodiesel. *Bulletin of Chemical Reaction Engineering & Catalysis*. 11 (1), 2016, 34-39. https://doi.org/10.9767/bcrec.11.1.413.34-39

Madhu, D. and Sharma, Y. C. (2017). Resource-Efficient Technologies Synthesis of a reusable novel catalyst (β -tricalcium phosphate) for biodiesel production from a common Indian tribal feedstock ☆. *Resource-Efficient Technologies*, *3*(2), 144–

157. https://doi.org/10.1016/j.reffit.2017.02.004

Mishra, A., Siddiqi, H., Kumari, U., Behera, I. D., Mukherjee, S., and Meikap, B. C. (2021). Pyrolysis of Waste Lubricating Oil/Waste Motor Oil to Generate High-Grade Fuel Oil: A comprehensive review. *Renewable and Sustainable Energy Reviews*, *150*(January), 111446. https://doi.org/10.1016/j.rser.2021.111446

Moses, K. K., Aliyu, A., Hamza, A. and Mohammed-Dabo, I. A. (2023). Recycling of waste lubricating oil: A review of the recycling technologies with a focus on catalytic cracking, techno-economic and life cycle assessments. *Journal of Environmental Chemical Engineering.* 11(2023) 111273. https://doi.org/10.1016/j.jece.2023.111273

Mousavi, S. S. A. H., Sadrameli, S. M. and Saeedi Dehaghani, A. H. (2022). Catalytic pyrolysis of municipal plastic waste over nano MIL-53 (Cu) derived @ zeolite Y for gasoline, jet fuel, and diesel range fuel production. *Process Safety and Environmental Protection*, *164*, 449–467. https://doi.org/10.1016/j.psep.2022.06.018

Najafi, G., Ghobadian, B., Yusaf, T., Mohammad, S. and Mamat, R. (2015). Optimization of performance and exhaust emission parameters of a SI (spark ignition) engine with gasoline e ethanol blended fuels using response surface methodology. *Energy*. 90 (2015). 1815 – 1829. https://doi.org/10.1016/j.energy.2015.07.004

Niu, X., Gao, J., Wang, K., Miao, Q., Dong, M., Wang, G., Fan, W., Qin, Z. and Wang, J. (2017)., Influence of crystal size on the catalytic performance of H-ZSM-5 and Zn/H-ZSM-5 in the conversion of methanol to aromatics. *Fuel Processing Technology.* **157.** 99 – 107. https://doi:10.1016/j.fuproc.2016.12.006

Pinheiro, C. T., Ascensão, V. R., Cardoso, C. M., Quina, M. J. and Gando-Ferreira, L. M. (2017). An Overview of Waste Lubricant Oil Management System: Physicochemical Characterization Contribution for its Improvement. *Journal of Cleaner Production*, *150*, 301–308. https://doi.org/10.1016/j.jclepro.2017.03.024

Prayogi, Y. and Sinaga, N. (2019). Performance and exhaust gas emission of gasoline engine fueled by gasoline, acetone and wet methanol blends. *Material Science and Engineering.* 535(2019). https://doi.org/10.1088/1757-899X/535/1/012013

Santhoshkumar, A. and Ramanathan, A. (2020). Recycling of waste engine oil through pyrolysis process for the production of

diesel like fuel and its uses in diesel engine. *Energy*. 197 (2020) 117240. https://doi.org/10.1016/j.energy.2020.117240

Sarathy, S. M., Farooq, A. and Kalghatgi, G. T. (2017). Recent progress in gasoline surrogate fuels. *Progress in Energy and Combustion Science*, *000*, 1–42. https://doi.org/10.1016/j.pecs.2017.09.004

Simsek, S. and Uslu, S. (2020). Investigation of the impacts of gasoline, biogas and LPG fuels on engine performance and exhaust emissions in di ff erent throttle positions on SI engine. *Fuel*, *279*(June), 118528. https://doi.org/10.1016/j.fuel.2020.118528

Suiuay, C., Laloon, K., Katekaew, S., Senawong, K., Noisuwan, P. and Sudajan, S. (2020). Effect of gasoline-like fuel obtained from hard-resin of Yang (Dipterocarpus alatus) on single cylinder gasoline engine performance and exhaust emissions. *Renewable Energy*, *153*, 634–645. https://doi.org/10.1016/j.renene.2020.02.036

Suiuay, C., Katekaew, S., Senawong, K., Junsiri, C., Srichat, A. and Laloon, K. (2023). Production of gasoline and diesel-like fuel from natural rubber scrap: Upgrading of the liquid fuel properties and performance in a spark ignition engine. *Energy*, *283*. https://doi.org/10.1016/j.energy.2023.128583

Veses, A., Puértolas, B., López, J. M., Callén, M. S., Solsona, B. and García, T. (2016)., Promoting Deoxygenation of Bio-Oil by Metal-Loaded Hierarchical ZSM-5 Zeolites. *ACS Sustainable Chemistry and Science.* **4.** 1653 – 1660. https://doi.org/10.1021/acssuschemeng.5b01606

Wei, J., Ge1, Q., Yao, R., Wen, Z., Fang, C., Guo, L., Xu, H. and Sun, J. (2017). Directly Converting CO_2 into a Gasoline Fuel. *Nature Communications.* 8:15174. DOI: 10.1038/ncomms15174. www.nature.com/naturecommunications.

Widayat, W and Annisa, A. N. (2016)., Synthesis and Characterization of ZSM-5 Catalyst at Different Temperatures. *IOP Conference Series: Materials Science and Engineering.* **214.** 012032. https://doi.10.1088/1757-899X/214/1/012032

Zandi-Atashbar, N., Ensafi, A. A. and Ahoor, A. H. (2017). Nano-CeO2/SiO2 as an Efficient Catalytic Conversion of Waste Engine Oil into Liquid Fuel. *Journal of Cleaner Production*, *166*, 1010–1019. https://doi.org/10.1016/j.jclepro.2017.08.103

Zhang, K., Cao, Q., Jin, L., Li, P. and Zhang, X. (2017). A Novel Route to Utilize Waste Engine Oil by Blending it With Water and Coal. *Journal of Hazardous Materials*, *332*, 51–58. https://doi.org/10.1016/j.jhazmat.2017.02.052